

RESEARCH NOTE

A spectral analysis of geoid undulation and gravity anomaly data computed with Pratt's isostasy theory applied to Moho depth variations in Fennoscandia

Tomas Nord and Lars E. Sjöberg

Royal Institute of Technology, Department of Geodesy, S-100 44 Stockholm, Sweden

Accepted 1992 March 31. Received 1992 March 30; in original form 1991 November 28

SUMMARY

The analysis shows that the spectra of geoid undulation (ΔN) and gravity anomaly (Δg) computed from the values implied by the OSU89B harmonic coefficients, degrees 4–100, Rapp & Pavlis (1990), do not fit the spectra of ΔN and Δg computed from values implied by a Pratt-type isostatic model applied to the Moho depth variations in Fennoscandia as suggested by Anderson (1984) and Marquart (1989). The magnitudes of the model spectra are that much larger than the OSU89B spectra that the relevance of the isostasy model is questionable.

Key words: Fennoscandia, geoid, isostatic, Moho.

1 INTRODUCTION

Marquart (1989) tried to model the geoidal undulation in Fennoscandia, with the variations in Moho depth (h_m) given by Meissner, Wever & Flüh (1987), using Pratt's hypothesis of isostatically compensated variable densities of masses below the boundary down to a compensation depth D . Specifically, Marquart (1989) used Anderson's (1984) formula for the geoid undulation generated by the Moho topography which, assuming a fixed density contrast between crust and mantle ($\rho_m - \rho_c$), reads:

$$\Delta N = \frac{\pi G}{\gamma} (\rho_m - \rho_c) D h_m, \quad (1)$$

where G is the gravitational constant and γ is mean surface gravity.

Marquart (1989) found that (with $\rho_c = 2700 \text{ kg m}^{-3}$ and $\rho_m = 3100 \text{ kg m}^{-3}$ and D adjusted to 80 km) the resulting geoid map agrees well with the geoid map determined from the potential coefficients of degrees 4 to 100 of the Rapp (1981) Earth Gravity Model. She concluded that the downward deflected Moho is the dominating source of the geoid undulation and not the post-glacial rebound.

However, Anderson (1984) and Marquart (1989) based their analysis of the correlation between geoid undulation and Moho depth variations on equation (1), which is an approximate formula consistent with a density contrast $\rho_m - \rho_c$ within an infinite plate of thickness h_m . The corresponding gravity anomaly is zero. Hence Sjöberg, Nord & Faan (1991) derived new surface integral formulae for the contributions to geoid undulation (ΔN) and free air gravity anomaly (Δg) from Moho depth variations (see Appendix). The resulting formulae are:

$$\Delta N = \frac{G(\rho_2 - \rho_1)}{\gamma} \sum_{n=0}^{\infty} \frac{1}{n+3} \iint_{\sigma} \left[\frac{D}{D+h_m} \frac{(R_m+h_m)^{n+3} - (R_m-D)^{n+3}}{R^{n+1}} - \frac{R_m^{n+3} - (R_m-D)^{n+3}}{R^{n+1}} \right] P_n(\cos \psi) d\sigma_i, \quad (2)$$

and

$$\begin{aligned} \Delta g &= -\gamma \frac{\partial \Delta N}{\partial R} - \frac{2\gamma \Delta N}{R} \\ &= G(\rho_2 - \rho_1) \sum_{n=0}^{\infty} \frac{n-1}{n+3} \iint_{\sigma} \left[\frac{D}{D+h_m} \frac{(R_m+h_m)^{n+3} - (R_m-D)^{n+3}}{R^{n+2}} - \frac{R_m^{n+3} - (R_m-D)^{n+3}}{R^{n+2}} \right] P_n(\cos \psi) d\sigma_i, \end{aligned} \quad (3)$$

or, approximately,

$$\Delta N = \frac{G(\rho_2 - \rho_1)D}{2\gamma} \sum_{n=0}^{\infty} \left(\frac{R_m}{R}\right)^{(n+1)} (n+2) \iint_{\sigma} h_m P_n(\cos \psi) d\sigma_i, \quad (4)$$

$$\Delta g = \frac{G(\rho_2 - \rho_1)D}{2R_m} \sum_{n=0}^{\infty} \left(\frac{R_m}{R}\right)^{(n+2)} (n-1)(n+2) \iint_{\sigma} h_m P_n(\cos \psi) d\sigma_i, \quad (5)$$

where R_m and R are the radii of mean Moho boundary and Earth's surface, respectively, and $P_n(\cos \psi)$ is the Legendre polynomial of degree n and geocentric angle ψ between the computation point and the integration point. h_m is the height (positive or negative) of the Moho boundary, with respect to its mean radius R_m . One advantage of these new formulae is that they permit the study of a selected spectral window of the geoidal undulation or gravity anomaly.

Using the Moho depth map of Luosto (1990) digitized into $294 0.5^\circ \times 2^\circ$ blocks in equations (2)–(3), Sjöberg *et al.* (1991) found that the magnitude of the resulting geoid map is heavily dependent on the choice of the arbitrary compensation depth D (cf. equations 4 and 5). Also when comparing the resulting geoid map with a map determined from the OSU89B Earth Gravity Model (degrees 4–100), Rapp & Pavlis (1990), the resulting residual map is far from zero. Sjöberg *et al.* (1991) therefore concluded that the Moho depth variation contributes little to the Fennoscandian geoid undulation.

In this study we take a different approach to the problem of determining the correlation between geoid undulation and Moho depth. We analyse the spectra of the already computed values for ΔN and Δg in the Sjöberg *et al.* (1991) paper and compare the result with the OSU89B spectra.

2 COMPUTATIONS

Sjöberg (1982) developed a numerical approximation for determining degree variances c_n of signal H :

$$c_n = \frac{2n+1}{16\pi^2} \sum_i H_i \sum_j H_j \iint_{\Delta\sigma_i} \iint_{\Delta\sigma_j} P_n(\cos \psi_{ji}) d\sigma_i d\sigma_j, \quad (6)$$

where H_i and H_j are (in this study) ΔN or Δg over surface elements $\Delta\sigma_i$ and $\Delta\sigma_j$. (Note that all values of ΔN and Δg outside the area of interest are set to zero.) For the multiple integral in (6) Sjöberg (1982) used the following approximation:

$$\iint_{\Delta\sigma_i} \iint_{\Delta\sigma_j} P_n(\cos \psi_{ji}) d\sigma_i d\sigma_j \approx \beta_n^2 P_n(\cos \psi_{ji}) \Delta\sigma_i \Delta\sigma_j, \quad (7)$$

where β_n are the eigenvalues of the mean value operator over a spherical cap of equal area (radius ψ_0) as $\Delta\sigma$:

$$\beta_n = \left(\frac{1}{1 - \cos \psi_0}\right) \left(\frac{1}{2n+1}\right) [P_{n-1}(\cos \psi_0) - P_{n+1}(\cos \psi_0)], \quad (8)$$

or, iteratively (Sjöberg 1980): $\beta_0 = 1$, $\beta_1 = (1 + t_0)/2$ and

$$\beta_n = \frac{2n-1}{n+1} t_0 \beta_{n-1} - \frac{n-2}{n+1} \beta_{n-2}; \quad n \geq 2, \quad (9)$$

where $t_0 = \cos \psi_0$. Combining (6) and (7) we get the final formula for degree variances:

$$c_n = \frac{2n+1}{16\pi^2} \beta_n^2 \sum_i H_i \Delta\sigma_i \sum_j H_j \Delta\sigma_j P_n(\cos \psi_{ji}). \quad (10)$$

The total power is given by:

$$\|H\|^2 = \sum_{n=0}^{\infty} c_n. \quad (11)$$

The numerical study is based on $0.5^\circ \times 2^\circ$ data blocks in Fennoscandia ($\phi_{\text{mean}} = 64.5^\circ$). Hence the area of such a block is approximately

$$\Delta\sigma = \frac{4\pi}{180} \cos \phi_{\text{mean}} \sin \frac{1^\circ}{4}, \quad (12)$$

and the radius ψ_0 of an equal area cap is given by

$$\Delta\sigma = 2\pi \int_0^{\psi_0} \sin \psi d\psi = 2\pi(1 - \cos \psi_0). \quad (13)$$

Equations (12) and (13) yields $\psi_0 \approx 0.37^\circ$.

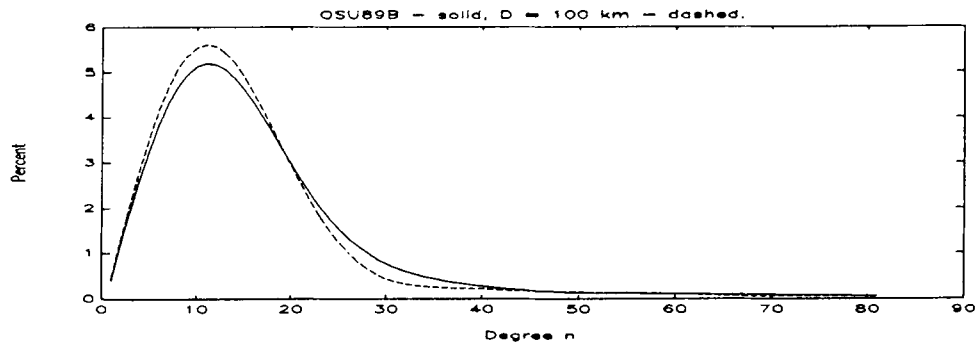


Figure 1. Percentage power spectra of geoidal undulation. Note that isostasy models $D = 50$ km and $D = 30$ km are almost identical to the one with $D = 100$ km.

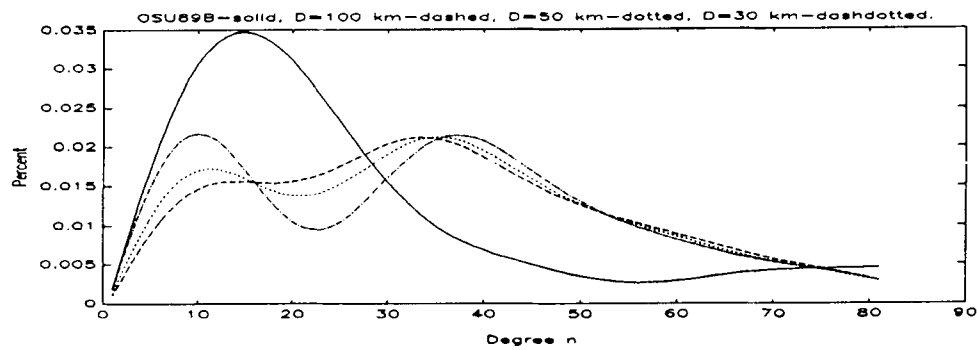


Figure 2. Percentage power spectra of gravity anomaly.

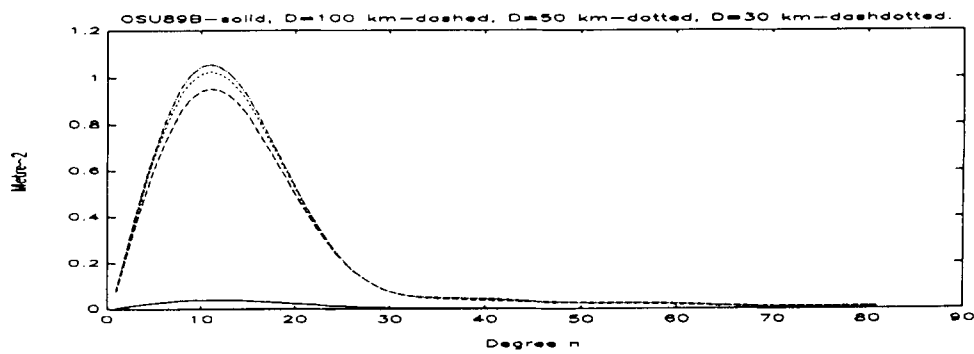


Figure 3. Magnitude of power spectra of geoidal undulation.

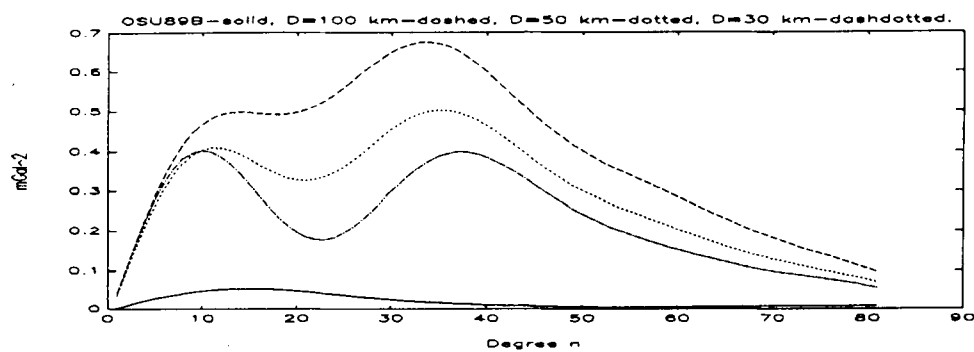


Figure 4. Magnitude of power spectra of gravity anomaly.

In Figs 1 (ΔN) and 2 (Δg) we present the percentage power spectra degree by degree for both the computed ΔN and Δg with the method derived in the Appendix (degrees 4–100) for the variational Moho depth, and ΔN and Δg computed with coefficients given by OSU89B (also degrees 4–100). Also, in Figs 3 and 4 the magnitude of c_n are presented.

3 CONCLUSIONS

The computations show that the magnitude of the isostatically modelled geoidal undulation contribution from the Moho density contrast does not fit the OSU89B data. The modelled gravity anomaly spectrum fits neither the magnitude nor the shape of the OSU89B spectrum. Subsequently, in contrast to the results of Anderson and Maquart, the conclusion must be that the Moho depth variation is not a major source of the geoid undulation and gravity anomaly in Fennoscandia. Although our computations were based on Anderson's isostatic model, the conclusion is expected to hold for any reasonable model of isostatic compensation.

ACKNOWLEDGMENTS

Mrs Jadwiga Osiatynska is acknowledged for digitizing the Moho depth data.

REFERENCES

- Anderson, A. J., 1984. Geophysical interpretations of features in marine geoid of Fennoscandia, *Mar. Geophys. Res.*, **7**, 191–203.
- Luosto, U., 1990. Seismic data from the northern segment of the EGT and from the nearby profiles, in *Proceedings of the Sixth Workshop on the European Geotraverse (EGT) Project*, pp. 53–63, eds Freeman, R. & Mueller, H., European Science Foundation, Strassbourg.
- Maquart, G., 1989. Isostatic topography and crustal depth corrections for the Fennoscandian geoid, *Tectonophysics*, **169**, 67–77.
- Meissner, R., Wever, T. H. & Flüh, E. R., 1987. The Moho in Europe—Implications for crustal development, *Ann. Geophys.*, **5B**, 357–364.
- Rapp, R. H., 1981. The Earth's gravity field to degree and order 180 using SEASAT altimeter data, terrestrial gravity data and other data, *The Ohio State University, Department Geodet. Sci. Rep. No. 322*.
- Rapp, R. H. & Pavlis, N. K., 1990. The development and analysis of geopotential coefficient models to spherical harmonic degree 360, *J. geophys. Res.*, **95**, B13, 21 885–21 911.
- Sjöberg, L. E., 1980. A recurrence relation for the β_n -function, *Bull. Géod.*, **54**, 69–72.
- Sjöberg, L. E., 1982. Studies on the land uplift and its implications on the geoid in Fennoscandia, *University of Uppsala, Department of Geodesy Rep. No. 14*.
- Sjöberg, L. E., Nord, T. & Faan, H., 1991. The Fennoscandian geoid bulge and its correlation with land uplift and Moho depth, *Presented to the symposium 'Application of Gravimetry and Space Techniques to Geodynamics and Ocean Dynamics'*, The XXth IUGG General Assembly, August 11–24, Vienna, Austria.

APPENDIX: DERIVATION OF INTEGRAL FORMULAE

The geoid undulation generated by the density contrasts at the Moho boundary and its compensation is composed of the primary component ΔN_1 and the effect of compensation ΔN_2 , i.e. $\Delta N = \Delta N_1 + \Delta N_2$. The total contributions to ΔN and Δg are divided into those from two regions: σ_1 with $h_m > 0$ and σ_2 with $h_m < 0$.

Case I (Region σ_1): $h_m > 0$.

Density contrasts:

$$\text{Primary: } \Delta \rho_1 = \frac{D}{D + h_m} (\rho_2 - \rho_1); \quad \text{Compensation: } \Delta \rho_2 = \frac{h_m}{D + h_m} (\rho_1 - \rho_2),$$

$$\Delta N_1 = \frac{T_1}{\gamma} = \frac{G}{\gamma} \iint_{\sigma_1} \int_{R_m}^{R_m + h_m} \frac{\Delta \rho_1 r_i^2 dr_i d\sigma_i}{\sqrt{r_i^2 + R^2 - 2r_i R \cos \psi}},$$

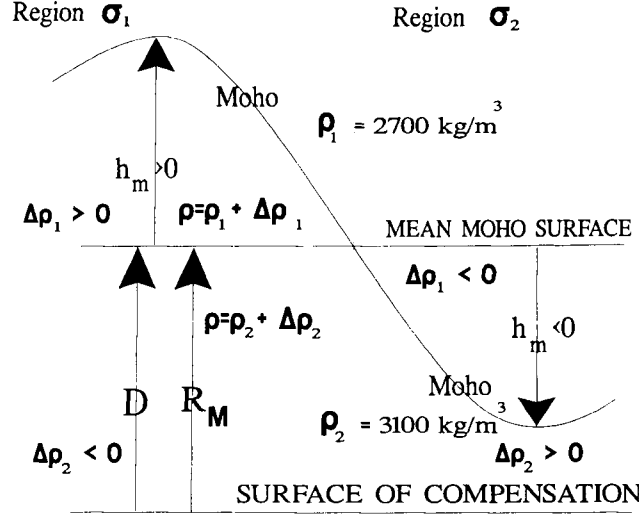


Figure A1. The computation model.

where G = gravitational constant, and γ = mean surface gravity.

$$\begin{aligned}\Delta N_1 &= \frac{G}{\gamma} \sum_{n=0}^{\infty} \iint_{\sigma_1} \int_{R_m}^{R_m+h_m} \frac{\Delta \rho_1 r_i^2}{R} \left(\frac{r_i}{R}\right)^n P_n(\cos \psi) d\sigma_i dr_i \\ &= \frac{G}{\gamma} \sum_{n=0}^{\infty} \iint_{\sigma_1} \frac{\Delta \rho_1}{n+3} \frac{(R_m+h_m)^{n+3} - R_m^{n+3}}{R^{n+1}} P_n(\cos \psi) d\sigma_i \\ &= \frac{G(\rho_2 - \rho_1)}{\gamma} \sum_{n=0}^{\infty} \frac{1}{n+3} \iint_{\sigma_1} \frac{D}{D+h_m} \frac{(R_m+h_m)^{n+3} - R_m^{n+3}}{R^{n+1}} P_n(\cos \psi) d\sigma_i,\end{aligned}\quad (A1)$$

$$\begin{aligned}\Delta N_2 &= \frac{T_2}{\gamma} = \frac{G}{\gamma} \iint_{\sigma_1} \int_{R_m-D}^{R_m} \frac{\Delta \rho_2 r_i^2 dr_i d\sigma_i}{\sqrt{r_i^2 + R^2 - 2r_i R \cos \psi}}, \\ \Delta N_2 &= \frac{G}{\gamma} \sum_{n=0}^{\infty} \iint_{\sigma_1} \int_{R_m-D}^{R_m} \frac{\Delta \rho_2 r_i^2}{R} \left(\frac{r_i}{R}\right)^n P_n(\cos \psi) d\sigma_i dr_i \\ &= \frac{G}{\gamma} \sum_{n=0}^{\infty} \iint_{\sigma_1} \frac{\Delta \rho_2}{n+3} \frac{R_m^{n+3} - (R_m-D)^{n+3}}{R^{n+1}} P_n(\cos \psi) d\sigma_i \\ &= \frac{G(\rho_1 - \rho_2)}{\gamma} \sum_{n=0}^{\infty} \frac{1}{n+3} \iint_{\sigma_1} \frac{h_m}{D+h_m} \frac{R_m^{n+3} - (R_m-D)^{n+3}}{R^{n+1}} P_n(\cos \psi) d\sigma_i,\end{aligned}\quad (A2)$$

$$\Delta N = \frac{G(\rho_2 - \rho_1)}{\gamma} \sum_{n=0}^{\infty} \frac{1}{n+3} \iint_{\sigma_1} \left[\frac{D}{D+h_m} \frac{(R_m+h_m)^{n+3} - (R_m-D)^{n+3}}{R^{n+1}} - \frac{R_m^{n+3} - (R_m-D)^{n+3}}{R^{n+1}} \right] P_n(\cos \psi) d\sigma_i, \quad (A3)$$

$$\begin{aligned}\Delta g &= -\gamma \frac{\partial \Delta N}{\partial R} - \frac{2\gamma \Delta N}{R} \\ &= G(\rho_2 - \rho_1) \sum_{n=0}^{\infty} \frac{n-1}{n+3} \iint_{\sigma_1} \left[\frac{D}{D+h_m} \frac{(R_m+h_m)^{n+3} - (R_m-D)^{n+3}}{R^{n+2}} - \frac{R_m^{n+3} - (R_m-D)^{n+3}}{R^{n+2}} \right] P_n(\cos \psi) d\sigma_i.\end{aligned}\quad (A4)$$

Case II (Region σ_2): $h_m < 0$.

Density contrasts:

Primary: $\Delta\rho_1 = (\rho_1 - \rho_2)$; Compensation: $\Delta\rho_2 = \frac{h_m}{D + h_m}(\rho_2 - \rho_1)$,

$$\begin{aligned}\Delta N_1 &= \frac{T_1}{\gamma} = \frac{G}{\gamma} \iint_{\sigma_2} \int_{R_m+h_m}^{R_m} \frac{\Delta\rho_1 r_i^2 dr_i d\sigma_i}{\sqrt{r_i^2 + R^2 - 2r_i R \cos \psi}}, \\ \Delta N_1 &= \frac{G}{\gamma} \sum_{n=0}^{\infty} \iint_{\sigma_2} \int_{R_m+h_m}^{R_m} \frac{\Delta\rho_1 r_i^2}{R} \left(\frac{r_i}{R}\right)^n P_n(\cos \psi) d\sigma_i dr_i \\ &= \frac{G}{\gamma} \sum_{n=0}^{\infty} \iint_{\sigma_2} \frac{\Delta\rho_1}{n+3} \frac{R_m^{n+3} - (R_m + h_m)^{n+3}}{R^{n+1}} P_n(\cos \psi) d\sigma_i \\ &= \frac{G(\rho_1 - \rho_2)}{\gamma} \sum_{n=0}^{\infty} \frac{1}{n+3} \iint_{\sigma_2} \frac{R_m^{n+3} - (R_m + h_m)^{n+3}}{R^{n+1}} P_n(\cos \psi) d\sigma_i, \quad (A5)\end{aligned}$$

$$\begin{aligned}\Delta N_2 &= \frac{T_2}{\gamma} = \frac{G}{\gamma} \iint_{\sigma_2} \int_{R_m-D}^{R_m+h_m} \frac{\Delta\rho_2 r_i^2 dr_i d\sigma_i}{\sqrt{r_i^2 + R^2 - 2r_i R \cos \psi}}, \\ \Delta N_2 &= \frac{G}{\gamma} \sum_{n=0}^{\infty} \iint_{\sigma_2} \int_{R_m-D}^{R_m+h_m} \frac{\Delta\rho_2 r_i^2}{R} \left(\frac{r_i}{R}\right)^n P_n(\cos \psi) d\sigma_i dr_i \\ &= \frac{G}{\gamma} \sum_{n=0}^{\infty} \iint_{\sigma_2} \frac{\Delta\rho_2}{n+3} \frac{(R_m + h_m)^{n+3} - (R_m - D)^{n+3}}{R^{n+1}} P_n(\cos \psi) d\sigma_i \\ &= \frac{G(\rho_2 - \rho_1)}{\gamma} \sum_{n=0}^{\infty} \frac{1}{n+3} \iint_{\sigma_2} \frac{h_m}{D + h_m} \frac{(R_m + h_m)^{n+3} - (R_m - D)^{n+3}}{R^{n+1}} P_n(\cos \psi) d\sigma_i, \quad (A6)\end{aligned}$$

$$\Delta N = \frac{G(\rho_2 - \rho_1)}{\gamma} \sum_{n=0}^{\infty} \frac{1}{n+3} \iint_{\sigma_2} \left[\frac{D}{D + h_m} \frac{(R_m + h_m)^{n+3} - (R_m - D)^{n+3}}{R^{n+1}} - \frac{R_m^{n+3} - (R_m - D)^{n+3}}{R^{n+1}} \right] P_n(\cos \psi) d\sigma_i, \quad (A7)$$

$$\begin{aligned}\Delta g &= -\gamma \frac{\partial \Delta N}{\partial R} - \frac{2\gamma \Delta N}{R} \\ &= G(\rho_2 - \rho_1) \sum_{n=0}^{\infty} \frac{n-1}{n+3} \iint_{\sigma_2} \left[\frac{D}{D + h_m} \frac{(R_m + h_m)^{n+3} - (R_m - D)^{n+3}}{R^{n+2}} - \frac{R_m^{n+3} - (R_m - D)^{n+3}}{R^{n+2}} \right] P_n(\cos \psi) d\sigma_i. \quad (A8)\end{aligned}$$

As the contribution from regions σ_1 and σ_2 are formally identical, the total contributions to ΔN and Δg are obtained simply by changing integration area σ_2 in (A7) and (A8) to $\sigma = \sigma_1 + \sigma_2$. From (A3) and (A4) and the expansion (for small x):

$$(1+x)^{n+3} = 1 + (n+3)x + (n+3)(n+2)\frac{x^2}{2} + O(x^3),$$

where x is h_m/R_m or D/R_m ; one obtains the first-order approximations:

$$\Delta N = \frac{G(\rho_2 - \rho_1)D}{2\gamma} \sum_{n=0}^{\infty} \left(\frac{R_m}{R}\right)^{(n+1)} (n+2) \iint_{\sigma} h_m P_n(\cos \psi) d\sigma_i, \quad (A9)$$

and

$$\Delta g = \frac{G(\rho_2 - \rho_1)D}{2R_m} \sum_{n=0}^{\infty} \left(\frac{R_m}{R}\right)^{(n+2)} (n-1)(n+2) \iint_{\sigma} h_m P_n(\cos \psi) d\sigma_i. \quad (A10)$$